Dynamic phase manipulation of vertical cavity surface emitting lasers via on-chip integration of microfluidic channels

Zhuangzhuang Zhao, Yiyang Xie, Guanzhong Pan, Peinan Ni, Qiuhua Wang, Yibo Dong, Liangchen Hu, Jie Sun, Hongda Chen, Chen Xu, et al.

Dynamic phase manipulation of vertical cavity surface emitting lasers via on-chip integration of microfluidic channels

Zhuangzhuang Zhao[1], Yiyang Xie[1,*], Guanzhong Pan[1], Peinan Ni[2,3*], Qiuhua Wang[1], Yibo Dong[1], Liangchen Hu[1], Jie Sun[1], Hongda Chen[4], Chen Xu[1,*], and Patrice Genevet[2,*]

[1]*Key Laboratory of Optoelectronics Technology, Ministry of Education, Beijing University of Technology, Beijing 100124, China*
[2] *Université Côte d'Azur, CNRS, Centre de Recherche sur l'Hétéro-Epitaxie et ses Applications (CRHEA), Valbonne, 06560, France*
[3] *Department of Physics, Baylor University, Waco, Texas 76798, United States*
[4] *State Key Laboratory of Integrated Optoelectronics, Institute of Semiconductor, Chinese Academy of Sciences, Beijing 100083, China*

[*]*Corresponding authors: xieyiyang@bjut.edu.cn; peinan_ni@baylor.edu; xuchen58@bjut.edu.cn; patrice.genevet@crhea.cnrs.fr*

Abstract: Vertical cavity surface-emitting lasers (VCSELs) have experienced a rapid development to become one of the key components for the development of the next generation of optoelectronic technologies. Dynamic phase manipulation of VCSELs within a compact system with low-power consumption is highly desired for a large variety of applications. In this work, we incorporate the emerging microfluidic technique into the conventional VCSELs through a monolithic integration approach, enabling dynamic phase control of lasing emissions with low power consumption and low thermal generation. As a proof of concept, a beam steering device is experimentally demonstrated by directly integrating microfluidic channel on a coherently coupled VCSELs array. The results show that the deflection angles of the laser beam from the chip can be tuned from 0^o to 2.4^o under the injection of liquids with different refractive index into the microchannel. This implementation of compact laser systems with real-time wavefront controllability, low power-consumption and low heat generation, holds great potentials in

various applications, including optical fiber communications, laser printing, optical sensing, directional displays, and ultra-compact light detection and ranging (LiDAR).

Keywords: Metasurfaces; VCSELs; Microfluidic channels; Optoelectronic integrations; Beam steering

Introduction:

Since the first demonstration of the continuous wave (*cw*) operation at the room temperature in 1988, vertical cavity surface emitting lasers (VCSELs) have grown into the most versatile laser sources for various applications, ranging from optical communications, portable electronics and instrumentation to laser manufacturing and sensing.[1-3] VCSELs play an indispensable role in the development of the next generation of optoelectronic technologies, due to their unique characteristics of low-power consumption, circular beam profile, high modulation speed, wafer-level testing, and ease of fabrication in dense two-dimensional arrays.[4-6] To expand into emerging markets and new applications, strong push toward higher performance and extended functionalities are needed.. In this context, beam control of VCSELs, which relies on the wavefront manipulation of the lasers, is highly desired. For instance, the bare single mode lasers suffer from the large divergence angle, which is usually in the range of 10^{o}-20^{o}.[7-9] Conventional refractive optical components have been widely integrated with VCSELs for beam shaping purposes. However, refractive optics, which rely on the accumulated phase during light propagation through media, are bulky and heavy, and particularly their integration requires a precise alignment process, which inevitably increases the volume and complexity of the system. To overcome these limitations, diffractive optical elements (DOEs), such as Dammann gratings and Fresnel lenses, which feature a reduced thickness comparable to the wavelength of light, are employed for the integration of VCSELs to improve the beam quality,[10, 11] while the efficiency of the DOEs dramatically drops at larger deflection angles due to the light shadowing effect.[12, 13] Recently, integration of VCSELs with artificial optical surfaces, such as metasurfaces, has demonstrated unprecedented capabilities of tailing both the phase and amplitude to produce

complex field patterns with subwavelength spatial resolution and ultra-compactness, which promises high performance wide-field applications.[14-16]

Nevertheless, it worth stressing that the current integration approaches only involve passive optical components, meaning that their capability to control the phase is static and remains fixed after manufacturing of the optical components. Dynamic phase manipulation of the laser beams, both spatially and temporally, are crucial for the advancement of a wide range of emerging applications, including directional displays, human-machine interactions, real time optical cytometry analysis, and beam steering in a light detection and ranging (LiDAR) system. For this purpose, mechanically controlled moving components have been widely incorporated into VCSELs system for beam steering applications, such as rotating mirror,[17] piezoelectric actuator,[18] and micro-electromechanical system (MEMS).[19] However, those approaches have several drawbacks, including low speed, short lifetime, and high manufacturing cost. In contrast, non-mechanical solutions, which do not contain any moving part, are strongly preferred due to their faster operation-speed and higher reliability. Nevertheless, traditional non-mechanical beam steering devices usually rely on a separated beam deflector component and a delicate alignment process, which results in a bulky and complex structure.[20-22] To solve this issue, liquid crystal optical phase array (LCOPA) was integrated with VCSELs to steer the laser beam in a non-mechanical way in a previous work.[23] However, the performance of the LCOPA based approach is strictly dependent on the precision of alignment between the linear polarization direction of the laser beam and the orientation of the nematic liquid crystal molecules due to their polarization dependent phase response. In particular, the lasing polarization direction of the oxide aperture confined VCSELs tends to switch to its orthogonal state at higher injection currents due to material birefringence and thermal dissipation, resulting in the malfunctioning of the LCOPA

approach. Moreover, to date, the non-mechanical beam steering methods are limited with electro-optical effect[24, 25] or electro-thermal effect[26, 27], which require extra voltages to drive the beam deflector, causing additional power consumption and serious thermal dissipation problems and increasing the complexity in the design of electrode contacts. For instance, even though the combination of liquid crystal with gradient-index photonic crystal has been utilized for beam steering, the large operation voltage increases the temperature of the liquid crystal parts and undermines the reliability of the device.

The recent advance of the combination of state-of-the-art laser technologies with microscopy within microfluidic environment has fueled a revolutionary development of the so-called lab-on-a-chip systems, which enables real-time observation, tracking and manipulation of cellular/molecular processes in a fast and compact manner with minimal energy consumption.[28-30] In this context, the beneficial characteristics of lasers, including their independence on electrical charges and their compatibility with the biological materials, make them particularly suitable for biological matters manipulations by exerting optical forces. In this work, we explore new prospective integration of semiconductor lasers with microfluidic chip and experimentally demonstrate dynamic phase manipulation of laser beams. Our results prove that the complete phase tuning of the laser beam (in the range of $[0, 2\pi]$) can be implemented under the injection of liquids with different refractive indices that is without external electrical bias. As a proof of concept, the capability of this approach to control the phase is further exploited to realize a beam steering device. To this end, microfluidic channels are integrated onto the coherently coupled VCSEL arrays. Experimentally we show that the deflection angles of the laser beam of this device can be tuned in the range from 0^o to 2.4^o by injecting liquids with different index. Our approach offers several advantages, including polarization independent optical response, free of

driving voltage and no additional heat generation, which is highly suitable for high power laser applications. Therefore, this work provides a feasible alternative to realize wavefront tunable lasers with compact size, low power-consumption and minimum heat generation, holding potential in various applications including optical fiber communications, laser printing, optical sensing, face recognition, directional displays, and LiDAR applications.

Results and Discussions:

Phase manipulation principle and device design

VCSELs (lasing wavelength at 850 nm) are processed into the mesa size of 6 μm×6 μm. During the fabrication of the VCSEL, microfluidic channels are directly integrated onto the laser surfaces, as depicted in Fig. 1(a). The fabrication process involves, first, a 6.5μm-thick PECVD grown SiO_2 layer which is introduced on the surface of VCSEL to electrically isolate the laser elements from the microfluidic channel. After that, a 300 μm-thick nickel (Ni) layer is deposited as a mask to etch the SiO_2 by the reactive ion etching (RIE) process. In this way, 6 μm deep and 200 μm wide microchannelsare directly defined into the SiO_2 layer. Note that the 0.5 μm thick SiO_2 layer is intentionally preserved after the etching, to serve as an insulating layer between the injected liquid and the electrodes of the VCSEL chip. Then, the Ni mask and the SiO_2 layer over the electrode pad of the VCSEL array are removed by wet etching. After that, the microfluidic channel is finalized by bonding a 3 mm thick polydimethylsiloxane (PDMS) layer in the dimension of 0.8 cm × 1 cm onto the top surface of SiO_2 layer, as illustrated in Fig. 1(b). Both import and export holes for the circulation of liquid are defined in the PDMS film, respectively. Finally, the VCSEL chip integrating the microfluidic channels is packaged onto a PCB for characterization (Fig. 1(c)).

The beam steering mechanism relies on addressing local phase changes $\Delta\emptyset$ imposed between adjacent lasers by adjusting the effective refractive index of the microchannels integrated above each laser element injecting liquids with different refractive indices (n_i). The phase retardation $\Delta\emptyset$ (n_1) can be quantified by the expression:

$$\Delta\emptyset(n_1) = \frac{2\pi h(n_1 \% \gamma)}{\lambda} \qquad (1)$$

where h is the height of the microchannel, γ represents the period of change in the refractive index when the phase difference changes periodically from -π to π, % is an operator for calculating the remainder. Figure 1(d) reveals that the phase change of the laser beam caused by the injection of liquids linearly dependents on the refractive index of the liquids and a complete 2π range phase modulation can be implemented by varying the refractive index of the injected liquids from 1.26 to 1.4. Therefore, the integration of microfluidic channels allows for dynamic phase manipulation of the individual laser element on the chip. It is worth pointing out that the phase control of using microfluidic channels belongs to a non-mechanical approach, which contains no moving-parts.

Microfluidic channels enabled voltage-free beam steering devices

The capability of the integrated microfluidic channel to dynamic control the phase of VCSEL can be employed for active beam shaping. As a proof of concept, a beam steering device is experimentally demonstrated, which is composed of in-phase coherently coupled VCSEL arrays (CCVAs) and integrated microfluidic channels. The characteristics of the in-phase CCVAs, including two-dimensional planar array, coherent single-mode emission, and uniform near-field intensity profile, make them promising candidates for the applications of directional laser systems via integration with optical phased arrays. For the simplest case, 1×2 coherent coupled

VCSELs array is integrated with microfluidic channels to form a one-dimensional beam steering device (Fig. 2(a)). For this purpose, 1×2 CCVAs were first fabricated into the mesa size of 6 μm×6 μm (see Supplementary Fig. S1 fabrication details). To satisfy maximum in-phase coupling efficiency between adjacent VCSELs, a 4μm spacing distance is chosen [31]. Moreover, the electrodes of each laser elements were defined separately to improve the yield of CCVAs (as shown in the left panel of Fig. 2(b)).Such layout of electrical contacts offers the advantages of better near-field uniformity and easier controllability over the coherence of the CCVAs by individually adjusting the injection currents of each elements. Prior to the integration of the microfluidic channels, we characterized the standalone room-temperature performance of the CCVAs, including the power (*P*)-current (*I*)-voltage (*V*) curves, emission spectral, far-field, and near-field intensity distributions. The measured *P-I-V* indicates a threshold current of 4.0 mA and a maximum optical power of 1 mW under the injection current of 12 mA (see Fig. S2(a)). Figure S2(b) shows the emission spectrum under the injection currents of I_{left} = 4.7 mA and I_{right} = 5.3 mA. The emission spectrum of the CCVAs confirms the single fundamental mode operation with a side mode suppression ratio of 24.3dB. The far-field intensity distributions of the CCVAs is experimentally measured at *Z*= 4.5cm (Fig. 2(c), left), which agrees well with the simulation results (Fig. 2(c), right). The in-phase operation condition of the array creates a center lobe with high side lobe suppression ratio [25], featuring reasonable diffraction of about 2.9°, as determined by the far-field measurement. Figure. 2(d) shows the line profiles of the emission intensity along the A-A' direction (indicated in the right panel of Fig. 2(b)) obtained both from measurements and numerical simulations, respectively. The divergence angle of the CCVAs is calculated to be 2.5°, in good agreement with the experimental result. Moreover, the laser facet intensity distribution of the CCVAs presents interference fringes sandwiched between the two

laser elements (Fig. 2(e)), confirming the in-phase operation of the CCVAs . Note that the in-phase versus out of phase condition can be adjusted by controlling the injection current in the two devices respectively.

To construct the beam steering device, microfluidic channel was defined directly above the left laser element of the CCVAs, and a pure 6 μm thick SiO_2 layer was placed above the right laser element of the CCVAs, as illustrated in Fig. 2(a). This configuration allows for the active tuning of the phase retardation of the emitting laser beam from the left element by injecting liquids into the microfluidic channel, while the beam from the right laser element of the chip experienced a constant phase delay imposed by the top SiO_2 layer. As a result, the phase difference ($\Delta\emptyset$)between these two coupled lasers can be modulated, which will modify their interference patterns, thus enabling a dynamic beam steering function. The deflection angle ($\Delta\theta$) of this chip under the injection of liquid with a given refractive index can be calculated by the expression:

$$\Delta\theta = \frac{\lambda\Delta\emptyset}{2\pi d} * \frac{180^\circ}{\pi} \qquad (2)$$

where *d* is the center distance between the adjacent laser elements. When $\Delta\emptyset$ is 0, that is the left and right VCSEL element are in-phase, the corresponding deflection angle ($\Delta\theta$) is 0°. When $|\Delta\emptyset|$ is π, reaching the maximum phase delay, we achieve the largest deflection angle ($\Delta\theta$) of this device of about 2.436°. Therefore, the deflection angle of this beam steering device can be tuned from -2.436° to 2.436° by controlling the phase difference from -π to π. Such beam steering mechanism is further confirmed by numerical simulations of the far-field emission distributions (see Supplementary Fig. S3). It can be seen that the deflection angle ($\Delta\theta$) of the laser beam increases from 0^o to 2.436^o when the phase different ($\Delta\emptyset$) between the left and the right laser

element varies from 0 to π, and oppositely from 0^o to -2.436^o when the phase different ($\Delta\emptyset$) changes from 0 to - π.

Figure 3 schematically depicts the programmable beam steering function of the laser chip uponselective injection different liquids into the microfluidic channel. Beam steering in the range from 0^o to 2.405^o is experimentally observed from this device (Fig. 4(a)), in good agreement with the simulation results. The deflection angles were measured by projecting the laser beam onto a white screen placed at *Z*=4.25 cm away from the surface of the laser chip, and the far field pattern is recorded by a CCD camera. The liquids are injected into the microchannel at a rate of 0.025mL/min by using a multi-channels micro-pump. During the measurement, the injection current of the array elements is fixed at I_{left} = 4.7 mA and I_{right} = 5.3 mA. DI water, 6% sucrose solution, 20% sucrose solution, isopropanol and 46% sucrose solution are selected as the injected liquids, respectively, which are able to impose a 2 π phase change on the left laser element according to Equation 1. Figure 4(a) shows far-field patterns under the injection of different liquids,proving that the central far-field lobe can be steered to different positions. The deflection angle under the injection of water is considered as the reference 0^o for the simplicity of the comparisons among different injecting liquids. In this way, the offset Δd of the center lobe of different solutions relative to water are calculated from the far-field patterns. The beam deflection angle $\Delta\theta$ at a given offset Δd of the center lobe, can be calculated by the expression:

$$\Delta\theta = \arctan\left(\frac{\Delta d}{L}\right) * \frac{\pi}{180} \qquad (3)$$

where L is the distance from the chip to the white screen. The deflection angles corresponding to different liquids are determined and shown in Fig. 4(a), respectively. Fig. 4 (b) shows angular intensity profiles of the emission beams. It can be seen that the deflection angle increases linearly

with increasing the refractive index of the injected liquid, and the maximum deflection angle of the experiment is 2.41°, in good agreement with the calculated value. It is worth pointing out that this beam steering chip doesn't rely on the electro-optical or thermo-optic effect, resulting in low power consumption and low heat production. Note that as liquids are constantly replaced through the microchannel, the device can dissipate considerable portions of heat generated by the VCSEL array, reducing the chip's heat accumulation and thus improving the reliability of the chip, which is beneficial for high power applications. Due to VCSEL birefringence, the polarization direction of the emitting beam tends to switch by 90^o at larger injection current, which has been widely observed from the VCSELs. Such polarization switching at larger operation current will cause problems for those polarization sensitive beam steering approaches. Since the phase manipulation enabled by the microfluidic channels doesn't depend on the polarization, the beam steering functions reported in this work will not be affected by the polarization switching. The stability of the beam steering device was evaluated by comparing the emission power and lasing spectra under the injection of different liquids, as shown in Fig. 4(d) and (e), respectively. We observed that the beam steering chip exhibits high power stability and wavelength stability under different injection liquids. On the other hand, since the refractive index of an unknown liquid can be determined by measuring the deflection angle, this device has the potential for detecting chemicals based on their refractive indices.

Conclusions:

Dynamic phase manipulation of the VCSEL beam is demonstrated by the monolithic integration of microfluidic channels, which allows for a complete ([0, 2π]) phase control. This work provides a new solution for beam shaping VCSELs. As a proof of concept, beam steering chip is experimentally demonstrated by directly integrating microfluidic channels on the top of

coherently coupled VCSEL array. Controlling the interference conditions between adjacent lasers is achieved by injecting liquids with different refractive indices in the channels, which results on deflecting the coherent superposition of the laser beam in the range from 0^o to 2.41^o. This phase control method offers several advantages over the other techniques as it is polarization independent, it requires no driving voltages, and it does not cause additional heat generation. Therefore, it will facilitate high power laser applications with simple design and high robustness. Our results open the door to the realization of compact laser systems with tunable wavefront, low power-consumption and low heat generation, which can find important applications in optical fiber communications, laser printing, optical sensing, face recognition, directional display and LiDAR applications.

Experimental Methods:

The fabrication details of the microfluidic channel integrated CCVAs can be found in the supplementary information. The *P-I-V* curves of the chip were measured under pulse wave condition with a duty cycle of 0.2% and a pulse frequency of 100 Hz. Optical spectrum analyzer (AQ 6370c) were used to measure the emission spectral of the chip and the near-field intensity distribution is recorded by using 50x microscope. The far-field beam profiles were characterized by the laser beam profiler (Spiricon SP620).

Acknowledgments

We acknowledge the financial support from the National Key R&D Program of China (2018YFA0209000), National Natural Science Foundation of China (61604007, 61774175, 61874145), the Beijing Natural Science Foundation (4172009, 4182012), and the Beijing Municipal Commission of Education (KM201810005029). P. Ni, and P. Genevet acknowledge

the financial support from European Research Council (ERC) under the European Union's Horizon 2020 research and innovation program (grant agreement FLATLIGHT No 639109).

Author contributions

Y.Y.X., P. N. N., C.X. and P.G conceived the idea and coordinated the experiment. H.D.C, C. X. and P. G. supervised the project. Z. Z. Z., G.Z.P, Q.H.W, Y.B.D, L.C.H. fabricated the samples. Z. Z. Z., Y. Y. X., G.Z.P, and Q.H.W. performed the measurement. Z. Z. Z., Y. Y. X., P. N. N., P. G. conducted numerical simulations and supported the experiment with theoretical analysis. Z. Z. Z., Y. Y. X., P. N. N., and P. G. performed data analysis. Y. Y. X. and P. N. N. wrote the first draft. All authors participated in improving the final version of the manuscript.

Author Information

The authors declare that they have no competing financial interests.

References:

1. Chase, C.; Rao, Y.; Hofmann, W.; Chang-Hasnain, C. J., 1550 nm high contrast grating VCSEL. *Optics express* **2010,** *18* (15), 15461-15466.

2. Larsson, A., Advances in VCSELs for communication and sensing. *IEEE Journal of selected topics in quantum electronics* **2011,** *17* (6), 1552-1567.

3. Haglund, Å.; Hashemi, E.; Bengtsson, J.; Gustavsson, J.; Stattin, M.; Calciati, M.; Goano, M. In *Progress and challenges in electrically pumped GaN-based VCSELs,* Semiconductor Lasers and Laser Dynamics VII, International Society for Optics and Photonics: 2016; p 98920Y.

4. Wolf, P.; Li, H.; Caliman, A.; Mereuta, A.; Iakovlev, V.; Sirbu, A.; Kapon, E.; Bimberg, D., Spectral efficiency and energy efficiency of pulse-amplitude modulation using 1.3 μm wafer-fusion VCSELs for optical interconnects. *Acs Photonics* **2017,** *4* (8), 2018-2024.

5. Stepniak, G.; Lewandowski, A.; Kropp, J.; Ledentsov, N.; Shchukin, V.; Ledentsov, N.; Schaefer, G.; Agustin, M.; Turkiewicz, J., 54 Gbit/s OOK transmission using single-mode VCSEL up to 2.2 km MMF. *Electronics Letters* **2016,** *52* (8), 633-635.

6. Seurin, J.-F.; Ghosh, C. L.; Khalfin, V.; Miglo, A.; Xu, G.; Wynn, J. D.; Pradhan, P.; D'Asaro, L. A. In *High-power high-efficiency 2D VCSEL arrays*, Vertical-Cavity Surface-Emitting Lasers XII, International Society for Optics and Photonics: 2008; p 690808.

7. Jung, C.; Jager, R.; Grabherr, M.; Schnitzer, P.; Michalzik, R.; Weigl, B.; Muller, S.; Ebeling, K. J., 4.8 mW singlemode oxide confined top-surface emitting vertical-cavity laser diodes. *Electronics Letters* **1997,** *33* (21), 1790-1791.

8. Martinsson, H.; Vukusic, J.; Grabberr, M.; Michalzik, R.; Jager, R.; Ebeling, K. J.; Larsson, A., Transverse mode selection in large-area oxide-confined vertical-cavity surface-emitting lasers using a shallow surface relief. *IEEE Photonics Technology Letters* **1999,** *11* (12), 1536-1538.

9. Zhou, D.; Mawst, L. J., High-power single-mode antiresonant reflecting optical waveguide-type vertical-cavity surface-emitting lasers. *IEEE Journal of Quantum Electronics* **2002,** *38* (12), 1599-1606.

10. Martinsson, H.; Bengtsson, J.; Ghisoni, M.; Larsson, A., Monolithic integration of vertical-cavity surface-emitting laser and diffractive optical element for advanced beam shaping. *IEEE Photonics Technology Letters* **1999,** *11* (5), 503-505.

11. Rastani, K.; Orenstein, M.; Kapon, E.; Von Lehmen, A., Integration of planar Fresnel microlenses with vertical-cavity surface-emitting laser arrays. *Optics letters* **1991,** *16* (12), 919-921.

12. Lalanne, P.; Astilean, S.; Chavel, P.; Cambril, E.; Launois, H., Design and fabrication of blazed binary diffractive elements with sampling periods smaller than the structural cutoff. *JOSA A* **1999,** *16* (5), 1143-1156.

13. Hessler, T.; Rossi, M.; Kunz, R. E.; Gale, M. T., Analysis and optimization of fabrication of continuous-relief diffractive optical elements. *Appl. Opt.* **1998,** *37* (19), 4069-4079.

14. Xie, Y.-Y.; Ni, P.-N.; Wang, Q.-H.; Kan, Q.; Briere, G.; Chen, P.-P.; Zhao, Z.-Z.; Delga, A.; Ren, H.-R.; Chen, H.-D., Metasurface-integrated vertical cavity surface-emitting lasers for programmable directional lasing emissions. *Nat. Nanotechnol* **2020,** *15*, 125-130.

15. Li, K.; Rao, Y.; Chase, C.; Yang, W.; Chang-Hasnain, C. J., Monolithic high-contrast metastructure for beam-shaping VCSELs. *Optica* **2018,** *5* (1), 10-13.

16. Seghilani, M. S.; Myara, M.; Sellahi, M.; Legratiet, L.; Sagnes, I.; Beaudoin, G.; Lalanne, P.; Garnache, A., Vortex Laser based on III-V semiconductor metasurface: direct generation of coherent Laguerre-Gauss modes carrying controlled orbital angular momentum. *Scientific reports* **2016,** *6*, 38156.

17. Matsuda, T.; Abe, F.; Takahashi, H., Laser printer scanning system with a parabolic mirror. *Appl. Opt.* **1978,** *17* (6), 878-884.

18. Fryslie, S. T.; Gao, Z.; Dave, H.; Thompson, B. J.; Lakomy, K.; Lin, S.; Decker, P. J.; McElfresh, D. K.; Schutt-Ainé, J. E.; Choquette, K. D., Modulation of coherently coupled phased photonic crystal vertical cavity laser arrays. *IEEE Journal of Selected Topics in Quantum Electronics* **2017,** *23* (6), 1-9.

19. Errando-Herranz, C.; Le Thomas, N.; Gylfason, K. B., Low-power optical beam steering by microelectromechanical waveguide gratings. *Optics Letters* **2019,** *44* (4), 855-858.

20. Smirnov, S.; Lioubtchenko, D. V.; Oberhammer, J., Single-walled carbon nanotube layers for millimeter-wave beam steering. *Nanoscale* **2019,** *11* (31), 14691-14697.

21. Gu, X.; Shimada, T.; Koyama, F., Giant and high-resolution beam steering using slow-light waveguide amplifier. *Optics Express* **2011,** *19* (23), 22675-22683.

22. Gu, X.; Shimada, T.; Fuchida, A.; Matsutani, A.; Imamura, A.; Koyama, F., Ultra-compact beam-steering device based on Bragg reflector waveguide amplifier with number of resolution points over 100. *Electronics letters* **2012,** *48* (6), 336-337.

23. Pan, G.; Xu, C.; Xie, Y.; Dong, Y.; Wang, Q.; Deng, J.; Sun, J.; Chen, H., Ultra-compact electrically controlled beam steering chip based on coherently coupled VCSEL array directly integrated with optical phased array. *Optics express* **2019,** *27* (10), 13910-13922.

24. Resler, D.; Hobbs, D.; Sharp, R.; Friedman, L.; Dorschner, T., High-efficiency liquid-crystal optical phased-array beam steering. *Optics letters* **1996,** *21* (9), 689-691.

25. Qin, S.; Liu, C.; Wang, J.; Chen, K.; Xu, J.; Fu, S.; Liu, D.; Ran, Y., Liquid crystal-optical phased arrays (LC-OPA)-based optical beam steering with microradian resolution enabled by double gratings. *Appl. Opt.* **2019,** *58* (15), 4091-4098.

26. Sun, J.; Timurdogan, E.; Yaacobi, A.; Hosseini, E. S.; Watts, M. R., Large-scale nanophotonic phased array. *Nature* **2013,** *493* (7431), 195-199.

27. Kwong, D.; Hosseini, A.; Zhang, Y.; Chen, R. T., 1× 12 Unequally spaced waveguide array for actively tuned optical phased array on a silicon nanomembrane. *Applied Physics Letters* **2011,** *99* (5), 051104.

28. Crespi, A.; Gu, Y.; Ngamsom, B.; Hoekstra, H. J.; Dongre, C.; Pollnau, M.; Ramponi, R.; van den Vlekkert, H. H.; Watts, P.; Cerullo, G., Three-dimensional Mach-Zehnder interferometer in a microfluidic chip for spatially-resolved label-free detection. *Lab on a Chip* **2010,** *10* (9), 1167-1173.

29. Godin, J.; Chen, C. H.; Cho, S. H.; Qiao, W.; Tsai, F.; Lo, Y. H., Microfluidics and photonics for Bio- System- on- a- Chip: A review of advancements in technology towards a microfluidic flow cytometry chip. *Journal of biophotonics* **2008,** *1* (5), 355-376.

30. Lin, S.; Zhu, W.; Jin, Y.; Crozier, K. B., Surface-enhanced Raman scattering with Ag nanoparticles optically trapped by a photonic crystal cavity. *Nano letters* **2013,** *13* (2), 559-563.

31. Pan, G.; Xie, Y.; Xu, C.; Xun, M.; Dong, Y.; Deng, J.; Sun, J., Large-scale proton-implant-defined VCSEL arrays with narrow beamwidth. *IEEE Electron Device Letters* **2018,** *39* (3), 390-393.

Figures:

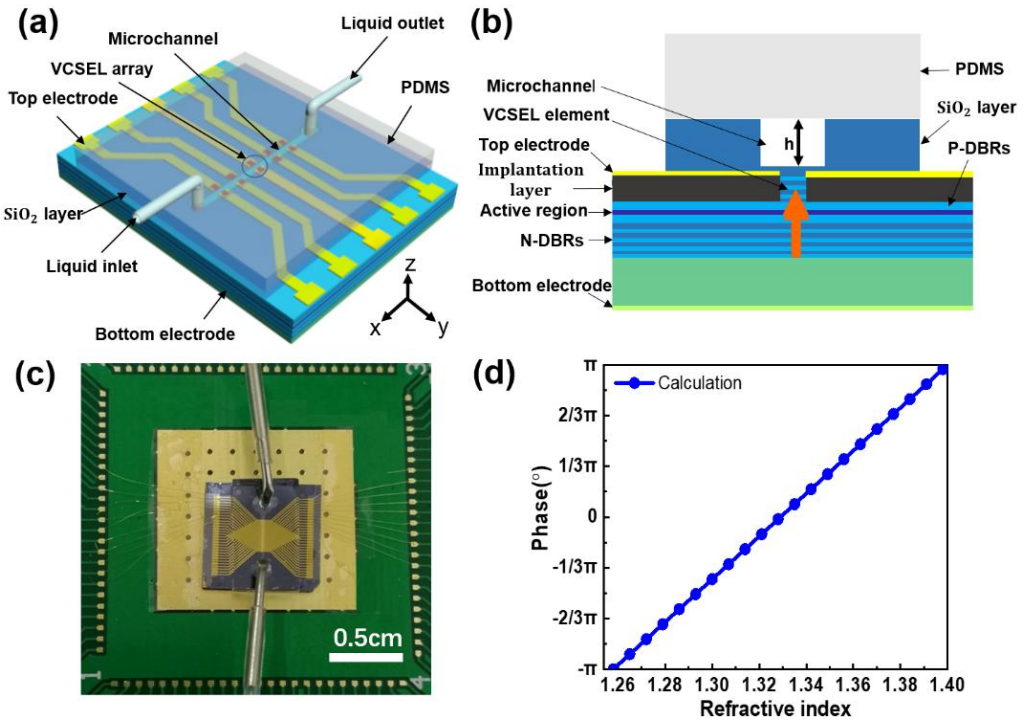

Figure 1. (a) The schematic illustration of the integration of microfluidic channel onto the top the emitting surface of a VCSELs chip to control the phase of the laser beam, and (b) represents the cross-section view; (c) The photo image of the integrated laser chip bonded to a PCB board for characterization; (d) The calculated phase delay imposed on the laser beam by the injection into the micro-channel of liquids with different refractive indices, showing that a complete 2π phase control is achievable with this design.

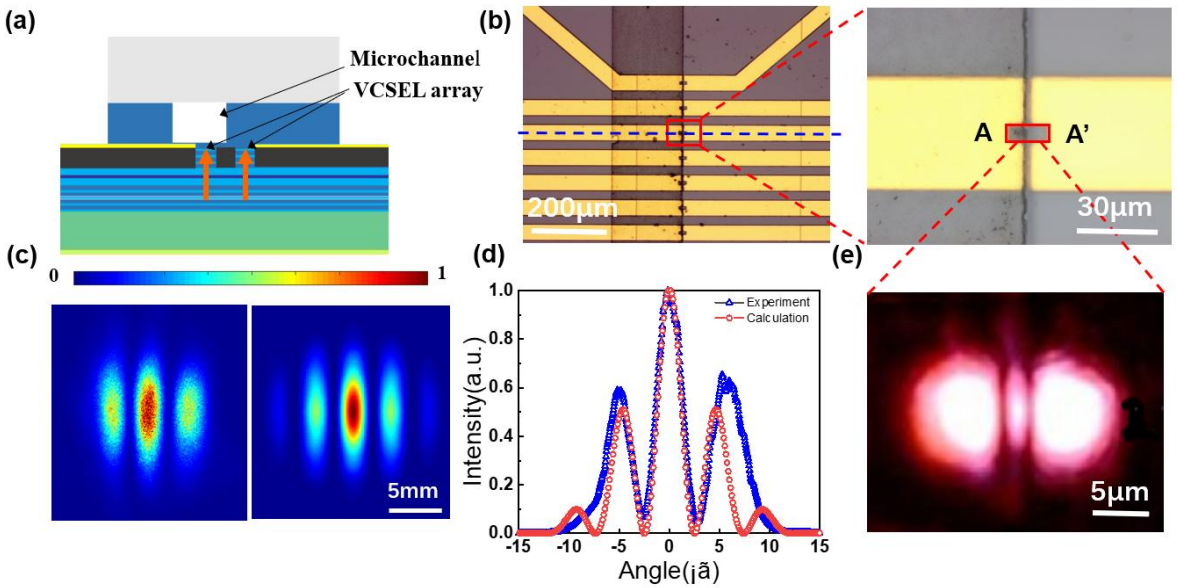

Figure 2. (a) The cross-section illustration of a beam steering device that is composed of 1×2 coherent coupled VCSELs array. A microfluidic channel is integrated on the top of the left laser element only and a SiO_2 is integrated on the top of the right laser element; (b) is the optical image of the beam steering device, and the inset shows a zoom-in area, where A and A' indicate the left and right laser elements, respectively. (c) The measured far-field intensity distributions (left) of the CCVAs agrees well with the simulation result (right), indicating the in-phase operation of the laser arrays; (d) The line profiles of the intensity distribution along A-A' direction; (e) The laser facets intensity pattern of the CCVAs shows the coupling fringe between the two laser elements.

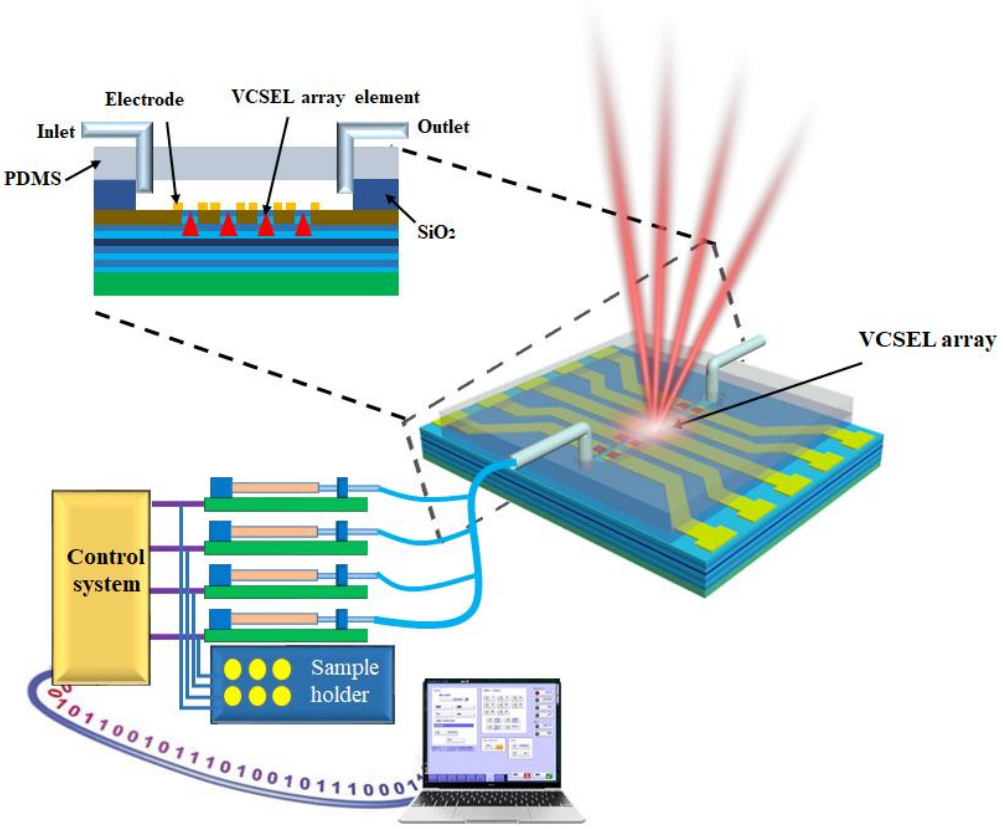

Figure 3. Schematic of the beam steering device depicting the operation principle of the programmable beam deflection function: liquids with different refractive indices can be selectively injected into the integrated microfluidic channel to tune the phase difference of the coupled lasers to deflect the emitted beam at different angles.

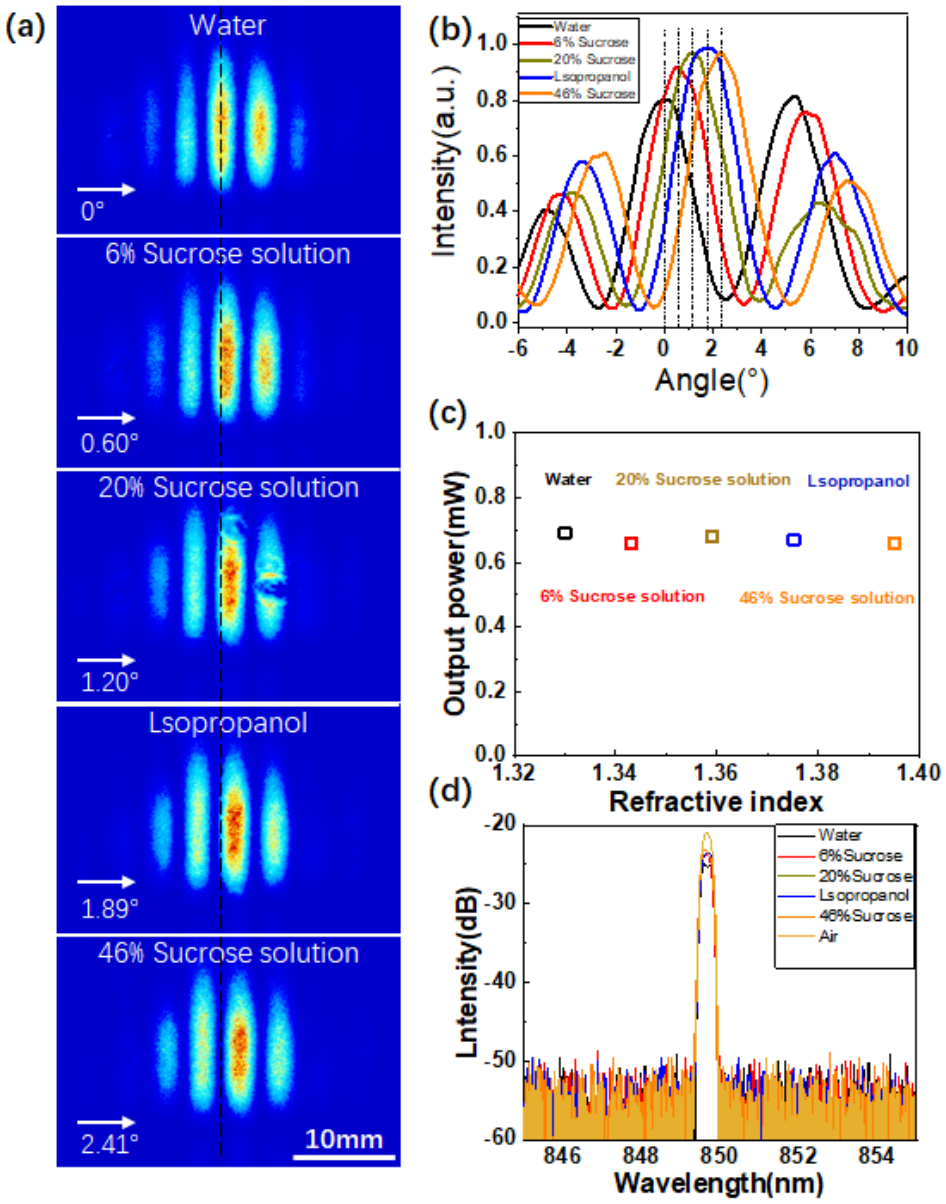

Figure 4. (a) Far-field intensity distribution for different injected solution in the micro-channel. The black dashed line indicates \theta=0(b) Angular profile of the emission intensity to compare the evolution upon injection of different liquids; The beam steering device shows comparable outpower (c) and emitting spectral (d) characteristics under the injection of different liquids, indicating the stability of the device.